Localization of Nanofibers on Polymer Surface Using Interface Transfer Technique

Vu Anh Doan, Shogo Nobukawa and Masayuki Yamaguchi*

School of Materials Science, Japan Advanced Institute of Science and Technology,

1-1 Asahidai, Nomi, Ishikawa, Japan.

* Corresponding author;

E-mail m_yama@jaist.ac.jp;

TEL +81-761-51-1621; FAX +81-761-51-1625

ABSTRACT:

A new method to localize polymer nanofibers on a polymer surface was verified using interface transfer technique of nanofibers between immiscible polymer pairs. Nanofibers of poly(butylene terephthalate) (PBT) were prepared in a molten polypropylene (PP) by melt stretching and subsequent quenching. The obtained composite of PP containing PBT nanofibers was compressed into a flat sheet and piled with a sheet of high-density polyethylene (HDPE). During annealing procedure of the piled sheets at the temperature between Tm's of PP and PBT, PBT nanofibers were transferred from PP to HDPE. Consequently, PBT fibers was confirmed on the surface of HDPE. Similarly, polytetrafluoroethylene (PTFE) nanofibers dispersed in a molten PLA, which were obtained by mechanical blending process, were found to move to PP during annealing procedure at the temperature between Tm's of PLA and PTFE. This movement leads to the modification of surface tension for PP. Furthermore, the piled sheets of PP/PBT and HDPE as well as those of PLA/PTFE and PP were easily separated each other because of the immiscible nature.

Keywords: A. Fibres; B. Interface/Interphase; B. Plastic deformation;

E. Surface treatments; Transfer technique.

1. Introduction

Numerous studies have been performed recently on modification of polymers by a small amount of nanofibers, because the addition of nanofibers having large surface area improves various properties including mechanical properties to a great extent [1-6]. Besides electro-spinning, a number of researches in recent years indicated that nanofibers can be prepared by simple techniques. For example, preparation of nanofibers of poly(butylene succinate) (PBS) in a molten poly(lactic acid) (PLA) was demonstrated by applied uniaxial stretching operation [7]. Ellison et al. [8] showed that poly(butylene terephthalate) (PBT), polypropylene (PP), and polystyrene (PS) nanofibers can be produced by melt blowing technique using a single orifice of melt blowing apparatus. Further, Chen et al. [9] established a polymer air-drawing model for melt-blown nanofibers of PBT. Borkar et al. [10] indicated that it is possible to fabricate polytetrafluoroethylene (PTFE) nano/microfibers both above and below its melting point with a high pressure jet of nitrogen or argon. Finally, Amran et al. [11] found that PTFE can be deformed into nanofibers in a molten PP by twin-screw extrusion process.

Because of outstanding properties such as flexibility, superior mechanical performance, and lightness, polymer nanofibers are optimal candidates as a filler of polymer composite fields [1-6]. Furthermore, localization of nanofillers on a surface is

one of the advanced methods for providing functional properties of a polymer surface, e.g., hydrophobicity.

In general, it is well-known that there are two approaches to modify the hydrophobicity of a surface; the one is to coat the surface by another material with low surface free energy and the other is increment of surface roughness [12]. Among polymeric materials, PTFE has attracted the attention of many researchers to modify the hydrophobicity of a solid surface, because it shows low surface energy and water-repellency in combination with other desirable properties such as chemical inertness and low frictional coefficient [13,14]. Hydrophobicity is usually measured by a contact angle of a water droplet [15]. In this study, the effect of existence of PTFE nanofibers on the surface free energy of PP was clarified by means of the contact angle method considering the roughness of PP surface.

In industry, the transfer technique, which can be considered as an imprinting lithography, is desired to locate nanofillers onto a solid surface because it requires only a small amount of nanofibers to modify the surface properties, leading to excellent cost-performance. Although various transfer techniques and/or nano-imprinting methods have been proposed by numerous research groups [16-19], only a few of them are relevant to nanofibers. Lee et al. [20] generated a large area of a bio-inspired

polymeric surface with nano-embosses or nanofibers using a nano-patterned aluminum sheet or a nanoporous anodic aluminum oxide, as a replication template in a nano-imprinting process. Romo-Uribe et al. [21] showed that polyamide nanofibers obtained by electro-spinning effectively reinforce polyanilin membranes. Chen et al. [22] applied microcontact printing, lithographic, and pattern-transfer methods to the transferring of randomly deposited polymethyglutarimide nanofibers with various diameters onto a glass substrate. In spite of the scientific interest, however, these methods have many difficulties to be applied in industry because of severe requirements of instruments and process.

Further, it should be noted that a new method to localize nanofillers on the surface of a polymer sheet was proposed using interface transfer of carbon nanotubes (CNT) in immiscible polymer pairs [23]. In the research, interface diffusion of CNTs from a PP/CNT composite to the surface of a PC sheet during the applied annealing was detected, in which Brownian motion as well as the compatibility with CNTs are the driving force of the immigration across the interface [24]. This phenomenon leads to the formation of conductive CNT network on PC surface with a considerably small amount of CNTs.

In this research, the interface transfer technique is developed to localize

nanofibers on a polymer surface.

2. Experimental

2.1 Materials

The polymers employed in this study were commercially available poly (butylene terephthalate) (PBT; Toray Industries, Inc., Japan; MFR = 26 [g/10min]; T_m (melting temperature) = 223 ^oC), two types of isotactic polypropylene (PP; Chisso Corporation, Japan; MFR = 20 and 11 [g/10min], T_m = 165 ^oC, denoted as PP-1 and PP-2, respectively), poly (lactic acid) (PLA; Toray Industries, Inc.; MFR = 22 [g/10min]; T_m = 152 ^oC), polytetrafluoroethylene (PTFE; Kitamura Co., Ltd, Japan; T_m = 346 ^oC), and high-density polyethylene (HDPE; Tosoh Corporation, Japan; MFR = 20 [g/10min], T_m = 135 ^oC).

2.2 Sample Preparation

PBT was dried under vacuum at 90 ºC for 4 h. Melt-mixing of PBT and PP-1 was performed using a 60 cc internal batch mixer for 3 min at 240 ºC, which is higher than the melting points of PP and PBT. The blend ratio of PP-1/PBT was 80/20 in weight fraction, and the blade rotation speed was 40 rpm. The blend was extruded at 240 ºC using a capillary rheometer. The extruded strand was subsequently stretched by a

set of rotating wheels and quenched immediately to obtain fibrous dispersion of PBT. A circular die employed has 20 mm in length and 1 mm in diameter. Further, the out-put rate was 0.007 cc/s and the draw ratio at the stretching process was 17. PP-1/PBT was kneaded again in the internal mixer at 200 ºC, which is lower than the melting point of PBT, to erase the orientation of PBT fibers. The obtained sample was compressed into flat sheets with a thickness of 1 mm using a laboratory compression-molding machine (Table-type test-press, Tester Sangyo Co., Ltd., Japan) at 200 ºC under 10 MPa for 3 min. HDPE sheets were also prepared using the compression-molding machine at 200 ºC under 10 MPa for 3 min. Then, the sheets were subsequently cooled at 30°C. After placing a pure HDPE sheet on the PP-1/PBT sheet, annealing treatment was conducted without pressure at 210 ºC for 5 min. After cooling, the piled sheets were separated. Because of the immiscible nature, the HDPE sheet was separated without any difficulty from the PP-1/PBT sheet.

Furthermore, PTFE and PLA were mixed together using the internal batch mixer with hindered phenol (Ciba, Irganox 1010, Chiyoda-Ku, Tokyo, Japan) and phosphate (Ciba, Irgafos 168) as thermal stabilizers at 180 ^{o}C for 3 min. The amount of each stabilizer was 0.5%. The blend ratio of PLA/PTFE was 80/20 in weight fraction and the blade rotation speed was 30 rpm. PLA/PTFE and PP-2 were also compressed

into flat sheets at 190 ^{o}C. The sheet of pure PP-2 was placed on the top of the sheet of a PLA/PTFE (80/20) composite. Then the piled sheets were annealed at 200 ^{o}C in the compression-molding machine without pressure for various residence times. A similar experiment was conducted for the pilled sheets composed of PP-2/PTFE and pure PLA at 210 ^{o}C. After cooling the sheets at 30 ^{o}C for 3 min, they were separated.

2.3 Measurements

The morphology of dispersed fibers was examined by a scanning electron microscope (SEM) (Hitachi, S4100). Prior to SEM observation, PP fraction was removed from the PP/PBT blend by xylene at 140 ^{o}C for 6 hours. Similarly, PLA fraction was removed from the PLA/PTFE blend by immersion in chloroform at room temperature for 16 hours. The metal-mash bags with the pore size of 20 μm were used to collect the undissolved part.

The surface morphology after the separation of the piled sheets as well as the fracture surface of a compressed PP-1/PBT (80/20) sheet were also checked by SEM. Prior to the observation, all specimens were coated with Pt–Pd by a sputter coating machine.

The attenuated total reflection (ATR) spectra of HDPE and HDPE/PBT composites were measured by a Fourier transform infrared spectroscopy (FT-IR) (Perkin Elmer, Spectrum 100) analyzer. The ratio between intensities of specific peaks of HDPE and PBT was calculated. In order to obtain reference samples to detect the amount of transferred PBT fibers, various HDPE/PBT blends containing 1, 3, 5, 10, and 20 wt. % of PBT were prepared by the internal batch mixer and compressed into sheets by the compression-molding machine.

The frequency dependence of oscillatory shear moduli in the molten state of PP-1 and HDPE was measured by a cone-and-plate rheometer (TA Instrument Ltd, AR2000ex) at the same temperature as the transfer experiment. Further, the zero-shear viscosities η_0 of the polymers were calculated by loss modulus as follows,

$$\eta_0 = \lim_{\omega \to 0} \left(\frac{G''}{\omega} \right) \qquad (1)$$

The surface free energy of PP was evaluated by means of contact angles between PP surface and triplet liquids including water, ethylene glycol, and diiodomethane following the VOCG (Van Oss-Chaudhry-Good) approach [25]. Surface roughness of the polymer sheets was also checked by scanning 20 μm in length employing a roughness tester (Time Group Inc., TR200).

3. Results and Discussion

3.1 Transfer of PBT nanofibers from PP/PBT to HDPE

Figure 1 shows the morphology of fracture surface of a compressed PP-1/PBT (80/20) sheet. Since PBT is immiscible with PP, the blend shows phase-separated morphology with spherical droplets of PBT. The average diameter of the droplets is approximately 2.8 μm, which is relatively smaller than those reported previously [26, 27]. The experimental conditions of melt-mixing and the viscosity ratio of the polymers will be responsible for the fine morphology.

[Fig.1]

Figure 2 shows the SEM image of the undissolved part in hot-xylene of the stretched PP-1/PBT sample. It is confirmed by DSC measurements (but not presented here) that PP is not contained in the undissolved part. Therefore, they are made of PBT. This is reasonable because PBT is not dissolved into hot-xylene. As seen in the figure, the present method can produce PBT fibers effectively.

The diameter of fibers was measured from the SEM pictures. As shown in Figure 3, the diameter of most PBT fibers is smaller than 1 μm, whereas the length is more than 100 μm. These results demonstrate that the volume of a PBT fiber is larger than that of a spherical particle, suggesting that PBT particles are coalesced together

inside the capillary rheometer, presumably by the constraction flow around the die entry. Moreover, the shear flow in the die land as well as the elongational flow at the die entry lead to the long fibers. The total shear strain in the die land is found to be 53 on average and the elongational strain (Hencky strain) at the die entry is approximately 4.5.

[Fig.2], [Fig.3]

In order to confirm the fiber transfer, ATR spectrum of the HDPE surface separated from PP-1/PBT was measured and presented in Figure 4. As shown in the figure, peaks around at 1120 cm^{-1} are detected for the separated HDPE, whereas pure HDPE shows no absorption peak in the wavenumber. The peak is ascribed to C-O stretching mode corresponding to trans-conformation of PBT chain [28, 29]. The results demonstrates that PBT fibers immigrate from PP phase to HDPE during annealing procedure at 210 ^{o}C for 5min.

For the purpose of quantitative evaluation of the amount of PBT fibers immigrated into HDPE surface during the annealing procedure, the calibration curve is produced using HDPE/PBT blends containing various amounts of PBT. The specific peaks employed are 1120 cm^{-1} and 1462 cm^{-1}. The latter is ascribed to CH_2 bending vibration mode of HDPE [30, 31]. The ratio of A_{1120} to A_{1462} is shown in Figure 5 as a calibration curve. It seems that the ratio is proportional to PBT concentration in the

blends. Therefore, the amount of PBT on the separated HDPE sheet is calculated based on the calibration curve. Because the ratio of A_{1120}/A_{1462} is 0.06 for the surface of HDPE after separation, it contains approximately 1.0 % of PBT fibers.

[Fig.4], [Fig.5]

3.2 Transfer of PTFE nanofibers from PLA/PTFE to PP

Figure 6 shows the undissolved part of the PLA/PTFE blend in chloroform. The figure demonstrates that PTFE particles are deformed into nanofibers with the diameter of approximately 100-500 nm by mixing with a molten PLA at 180 ^{o}C. This is a similar result to that reported by Amran et al. [11,32] employing PP as a matrix polymer. According to Amran et al. [32], PTFE particles are excluded from a molten PP due to the immiscibility, and form agglomeration with reorganization of crystallites. During shear flow, the agglomerated particles are fragmented into nanofibers by hydrodynamic force even below the melting point of PTFE. This peculiar morphology development is attributed to the loose packing of PTFE crystals.

[Fig.6]

The annealing procedure was carried out for the piled sheets comprising of pure PP-2 and PLA/PTFE (80/20). In order to clarify the distribution of PTFE nanofibers on

the surface of the separated PP-2 sheet, SEM observation is performed as shown in Figure 7. As seen in the figure, PTFE fibers are located randomly on the surface of PP-2. Further, the density of PTFE fibers on the surface remarkably increases with increasing the annealing time. This is reasonable because Brownian motion is required for the interface diffusion.

[Fig.7]

As compared with PBT fibers, the transfer phenomenon of PTFE fibers is more obvious. This can be explained by the difference in the diffusion constant. According to Doi and Edwards [33], the transformation diffusion constant of a rigid rod D_{tr} is derived by the following equation:

$$D_{tr} = \frac{k_B T \ln(L/d)}{2\pi\eta_m L} \qquad (2)$$

whrere k_B the Boltzman constant, d the diameter of a rigid rod, L the length of long axis, and η_m the viscosity of the medium.

Since the equation (2) is proposed for a rigid fiber, it cannot be used for flexible fibers directly. However, diffusion constants of both fibers are calculated following the equation to obtained rough information on the difference between them.

In this research, the zero-shear viscosity of PP-1 at the temperature of transfer experiment is approximately 2000 (Pa.s) and that of HDPE is 525 (Pa.s). Furthermore,

almost 50 % of PBT fibers is found to be approximate 800 nm in diameter and more than 300 μm in length. On the contrary, the diameter of most PTFE fibers is approximately 200 nm and the length is shorter than 30 μm. As a result, the diffusion constant of PTFE fibers is at least two times larger than that of PBT.

The annealing treatment is also carried out for the piled sheets comprising of pure PLA and PP-2/PTFE following the same procedure. Although, the size of fibers is almost the same, the immigration of the nanofibers does not occur in this system. It will be attributed to the difference in compatibility. Since the solubility parameter of PTFE, PP, and PLA are 12.7, 18.8, and 21.0 ($MPa^{1/2}$), respectively [34, 35], the compatibility of PTFE with PP is better than that with PLA. A similar phenomenon was observed by Zhang et al. in the blends of HDPE/PMMA and HDPE/PP containing vapor growth carbon nanofibers (VGCFs) [36]. According to them, VGCFs are found to be selectively located in HDPE phase because of the difference in the compatibility with VGCF.

The surface free energy is presented in Table 1 with the data of surface roughness, which is defined as the arithmetic mean of the absolute values of profile deviation from the mean value. The data shows that the surface free energy of PP-2 decreases with increasing the annealing time. Considering that the roughness of PP-2

surface is independent of the annealing time, the reduction of the surface free energy after annealing is owing to not only the change of roughness but also the increase in the density of PTFE fibers.

[Table 1]

4. Conclusion

A new method to localize nanofibers on a polymer sheet is presented using the interface transfer technique. This study also shows that PBT can be deformed into nanofibers in a molten PP by applied melt-stretching process. Furthermore, PBT nanofibers in a molten PP are transferred and localized on HDPE surface during annealing procedure at the temperature between Tm's of PP and PBT.

Similarly, this study also found that PTFE can be deformed into nanofibers in a molten PLA by simple mechanical blending procedure at lower temperature than T_m of PTFE. In addition, PTFE nanofibers are transferred from PLA to PP during annealing procedure in piled sheets comprising of PP and PLA/PTFE at the temperature between Tm's of PLA and PTFE. The localization of PTFE nanofibers leads to the reduction of surface free energy of PP. On the contrary, PTFE transfer does not occur from PP to PLA. This results indicate that the transfer phenomenon is affected by the compatibility with nanofibers. Since Brownian motion is needed for the interface transfer, the resident

time also affects the amount of the fibers.

References

1. Z. M. Huang, Y-Z. Zhang, M. Kotani and S. Ramakrishna, A review on polymer nanofibers by electrospinning and their application in nanocomposites. *Compos Sci Technol* **63** (2003), pp. 2223-2253.
2. I. Kang, Y. Y. Heung, J. H. Kim, J. W. Lee, R. Gollapudi, S. Subramaniam, S. Narasimhadevara, D. Hurd, G. R. Kirikera, V. Shanov, M. J. Schulz, D. Shi, J. Boerio, S. Mall and M. Ruggles-Wren, Introduction to carbon nanotube and nanofiber smarts materials, *Composites: Part B* **37** (2006), pp. 382-394.
3. G. G. Tibbetts, M. L. Lake, K. L. Strong and B. P. Rice, A review of the fabrication and properties of vapor-grown carbon nanofiber/polymer composites, *Compos Sci Technol* **67** (2007), pp. 1709-1718.
4. M. H. Al-Saleh and U. Sundararaj, A review of vapor grown carbon nanofiber/polymer conductive composites, *Carbon* **47** (2009), pp. 2-22.
5. A. J. Rodriguez, M. E. Guzman, C-S. Lim and B. Minaie, Mechanical properties of carbon nanofiber/fiber-reinforced hierarchical polymer composites manufactured with multiscale-reinforcement fabrics, *Carbon* **49** (2011), pp. 937-948.
6. F. Dalmas, J. Y. Cavaillé, C. Gauthier, L. Chazeau and R. Dendievel, Viscoelastic behavior and electrical properties of flexible nanofiber filled polymer nanocomposites. Influence of processing conditions, *Compos Sci Technol* **67** (2007), pp. 829-839.
7. T. Yokohara, K. Okamoto and M. Yamaguchi, Effect of the shape of dispersed particles on the thermal and mechanical properties of biomass polymer blends composed of poly(L-lactide) and poly(butyrate succinate), *J Appl Polym Sci* **117** (2010), pp. 2226-2232.

8. C. J. Ellison, A. Phatak, D. W. Giles, C. W. Macosko and F. S. Bates, Melt blown nanofibers: fiber diameter distributions and onset of fiber breakup, *Polymer* **48** (2007), pp. 3306-3316.
9. T. Chen, L. Li and X. Huang, Fiber diameter of polybutylene terephthalate melt-blown nonwovens, *J Appl Polym Sci* **97** (2005), pp. 1750-1752.
10. S. Borkar, B. Gu, M. Dirmyer, R. Delicado, A. Sen, B. R. Jackson and J. V. Badding, Polytetrafluoroethylene nano/microfibers by jet blowing, *Polymer* **47** (2006), pp. 8337-8343.
11. M. Amran, K. Okamoto and M. Yamaguchi, Rheological properties of polypropylene modified by polytetrafluoroethylene, *J Polym Sci B* **47** (2009), pp. 2008-2014.
12. P. N. Manoudis, I. Karapanagiotis, A. Tsakalof, I. Zuburtikudis and C. Panayiotou, Superhydrophobic composite films produced on various substrates, *Langmuir* **24** (2008), pp. 11225-11232.
13. P. Roach, N. J. Shirtcliffe and M. I Newton, Progress in superhydrophobic surface development, *Soft Matter* **4** (2008), pp. 224-240.
14. S. R. Coulson, I. Woodward, J. P. S. Badyal, S. A. Brewer and C. Willis, Super-repellent composite fluoropolymer surfaces, *J Phys Chem B* **104** (2000), pp. 8836-8840.
15. D. K. Owens and R. C. Wendt, Estimation of surface free energy of polymer, *J Appl Polym Sci* **13** (1969), pp. 1741-1747.
16. A. D. Campo and E. Arzt, Fabrication approaches for generating complex micro- and nanopatterns on polymeric surface, *Chemical Review* **108** (2008), pp. 911-945.

17. B. D. Gates, Q. Xu, M. Steward, D. Ryan, C. G. Willson and G. M. Whitesides, New approaches to nanofabrication: molding, printing and other techniques, *Chemical Review* **105** (2005), pp. 1171-1196.
18. L. J. Guo, Nanoimprint lithography: methods and material requirements, *Adv Mater* **19** (2007), pp. 495-513.
19. Z. Nie and E. Kumacheva, Patterning surfaces with functional polymers, *Nature Materials* **7** (2008), pp. 277-290.
20. W. Lee, M-K. Jin, W-C. Yoo and J.-K. Lee, Nanostructuring of a polymeric substrate with well-defined nanometer-scale topography and tailored surface wettability, *Langmuir* **20** (2004), pp. 7665-7669.
21. A. R. Uribe, L. Arizmendi, M. E. Romeo-Gruzmán, S. Sepúlveda-Guzmán and R. Cruz-Silva, Electrospun nylon nanofibers as effective reinforcement to polyaniline membranes, *Appl Mater Interface* **1** (2009), pp. 2502-2508.
22. J. Shi, L. Wang and Y. Chen, Microcontact printing and lithographic patterning of electrospun nanofibers, *Langmuir* **25** (2009), pp. 6015-6018.
23. H. Yoon, K. Okamoto and M. Yamaguchi, Carbon nanotube imprinting on a polymer surface, *Carbon* **47** (2009), pp. 2840-2846.
24. H. Yoon, K. Okamoto, K. Umishita and M. Yamaguchi, Development of conductive network of multiwalled carbon nanotubes in polycarbonate melt, *Polym Comp* **32** (2011), pp. 97-102.
25. C. J. V. Oss, R. J. Good, M. K. Chaudhury, The role of Van der Waals force and hydrogen bonds in “Hydrophobic interactions” between biopolymers and low energy surfaces, *J Colloid Interface Sci* **111** (1986), pp. 378-390.

26. B. Y. Zhang, Q. J. Sun, Q. Y. Li and Y. Wang, Thermal, morphology and mechanical characteristics of Polypropylene/polybutyrene terephthalate blends with a liquid crystalline polymer and ionomer, *J Appl Polym Sci* **102** (2006), pp. 4712-4719.
27. K. L. Børve, H. K. Kotlar and C. -G. Gustafson, Polypropylene-phenol formaldehyde-based compatibilizers. III. Application in PP/PBT and PP/PPE blends, *J Appl Polym Sci* **75** (2000), pp. 361-370.
28. J. M. Park, J. Y. Lee and Y. H. Park, Eco-friendly flame retardant Poly(butylene terephthalate) copolymer with thermal stability and hydrolytic resistance, *Macromolecular Research* **18** (2010), pp. 539-544.
29. J. Jang, J. H. Oh and S. I. Moon, Crystallization behavior of poly(ethylene terephthalate) blended with hyperbranched polymers: the effect of terminal groups and composition of hyperbranched polymers, *Macromolecules* **33** (2000), pp. 1864-1870.
30. C. J. Pouchert, *The Aldrich library of FT-IR spectroscopy* **2**, Library of Congress, USA (1985), pp. 1157.
31. E. Agosti, G. Zerbi and I. M. Ward, Structure of the skin and core of ultradrawn polyethylene films by vibrational spectroscopy, *Polymer* **33** (1992), pp. 4219-4229.
32. M. Amran, S. Nobukawa and M. Yamaguchi, Morphology Development of Polytetrafluoroethylene by Shear Flow in a Molten Polypropylene, *Pure Appl Chem.*, in press.
33. M. Doi and S. F. Edwards, *The Theory of Polymer Dynamic*, Oxford University Press, Oxford (1986), pp. 289-323.
34. J. E. Mark, *Physical Properties of Polymer Handbook* (2nd ed.), Springer Verlag, New York (2007), pp. 289-304.

35. U. Siemann, The Solubility parameter of Poly(DL-latic acid), *Eur Polym J* **28** (1992), pp. 293-297.
36. C. Zhang, P. Wang, C. Ma, G. Wu and M. Sumita, Temperature and time dependence of conductive network formation: Dynamic percolation and percolation time, *Polymer* **47** (2006), pp. 466-473.

Figure Captions

Figure 1 SEM image of the fractured surface of PP/PBT (80/20).

Figure 2 SEM image of the undissolved part in hot-xylene of PP/PBT after stretching.

Figure 3 Distribution of diameter for PBT fibers.

Figure 4 ATR spectra of (a) HDPE surface separated from PP/PBT and (b) pure HDPE.

Figure 5 Peak ratio of A_{1120} to A_{1462} plotted against PBT content in HDPE/PBT blends.

Figure 6 SEM image of the undissolved part in hot-xylene of PLA/PTFE.

Figure 7 SEM images of PP surface separated from PLA/PTFE after annealing for (a) 5 min and (b) 30 min.

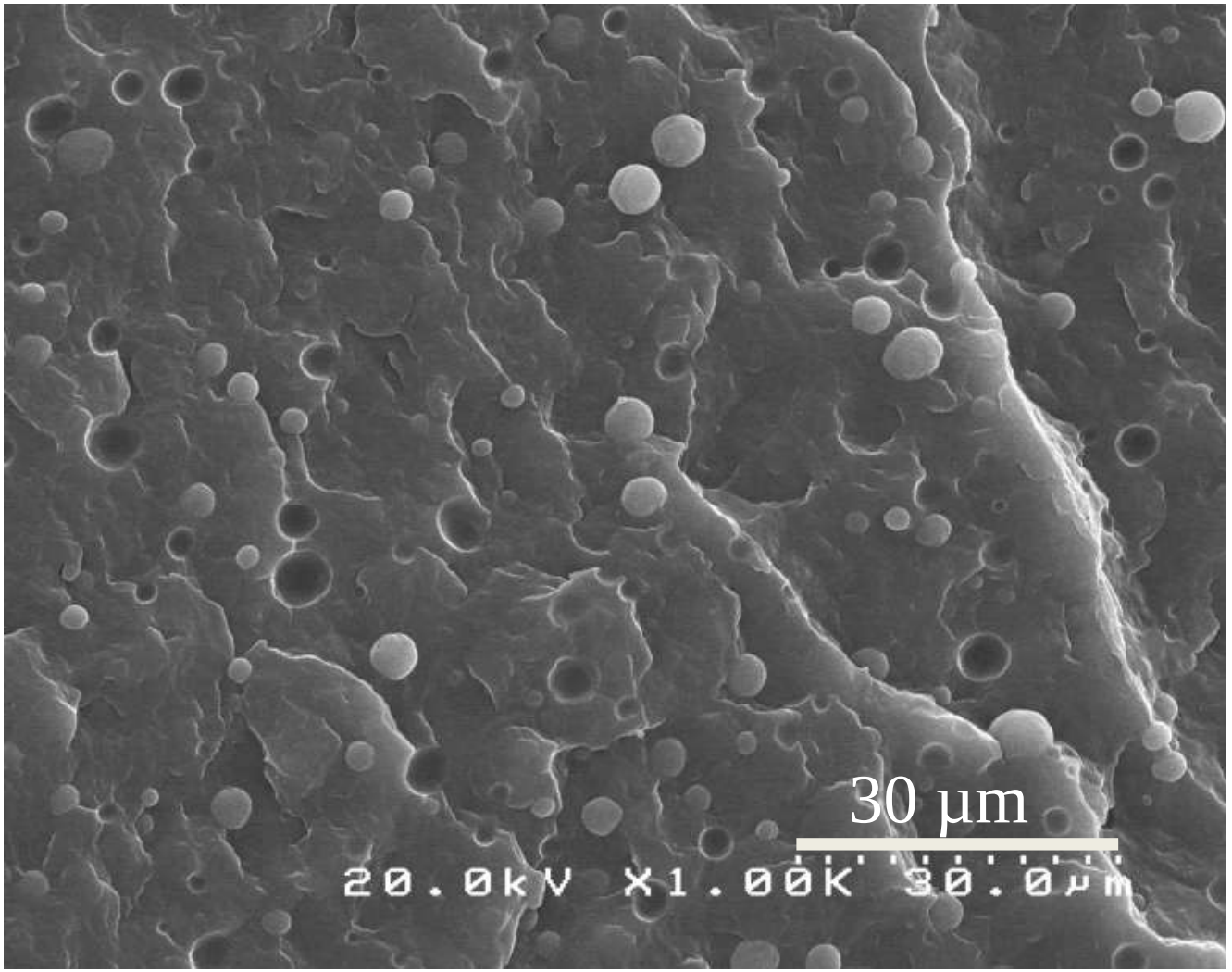

Figure 1

Vu and Yamaguchi

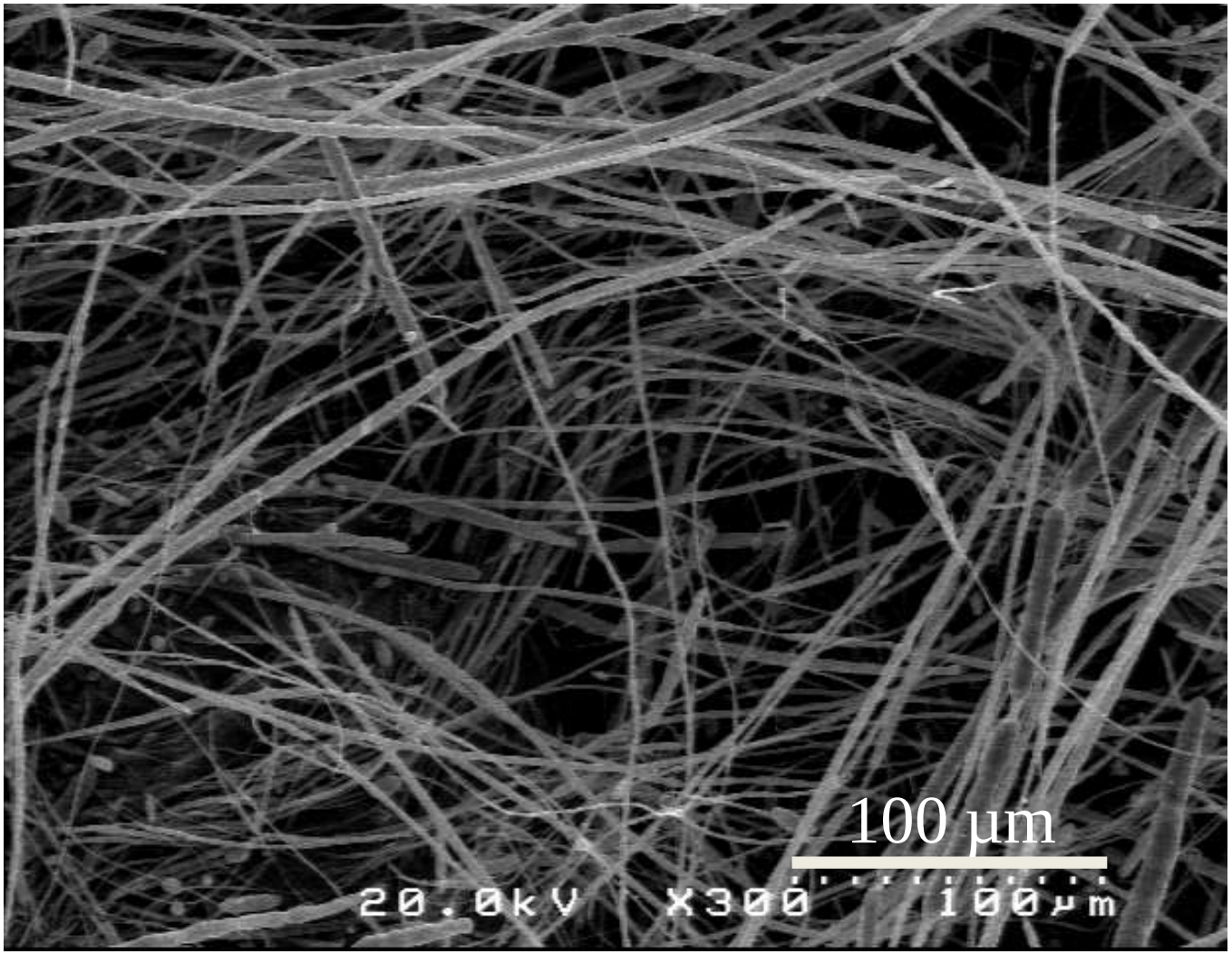

Figure 2

Vu and Yamaguchi

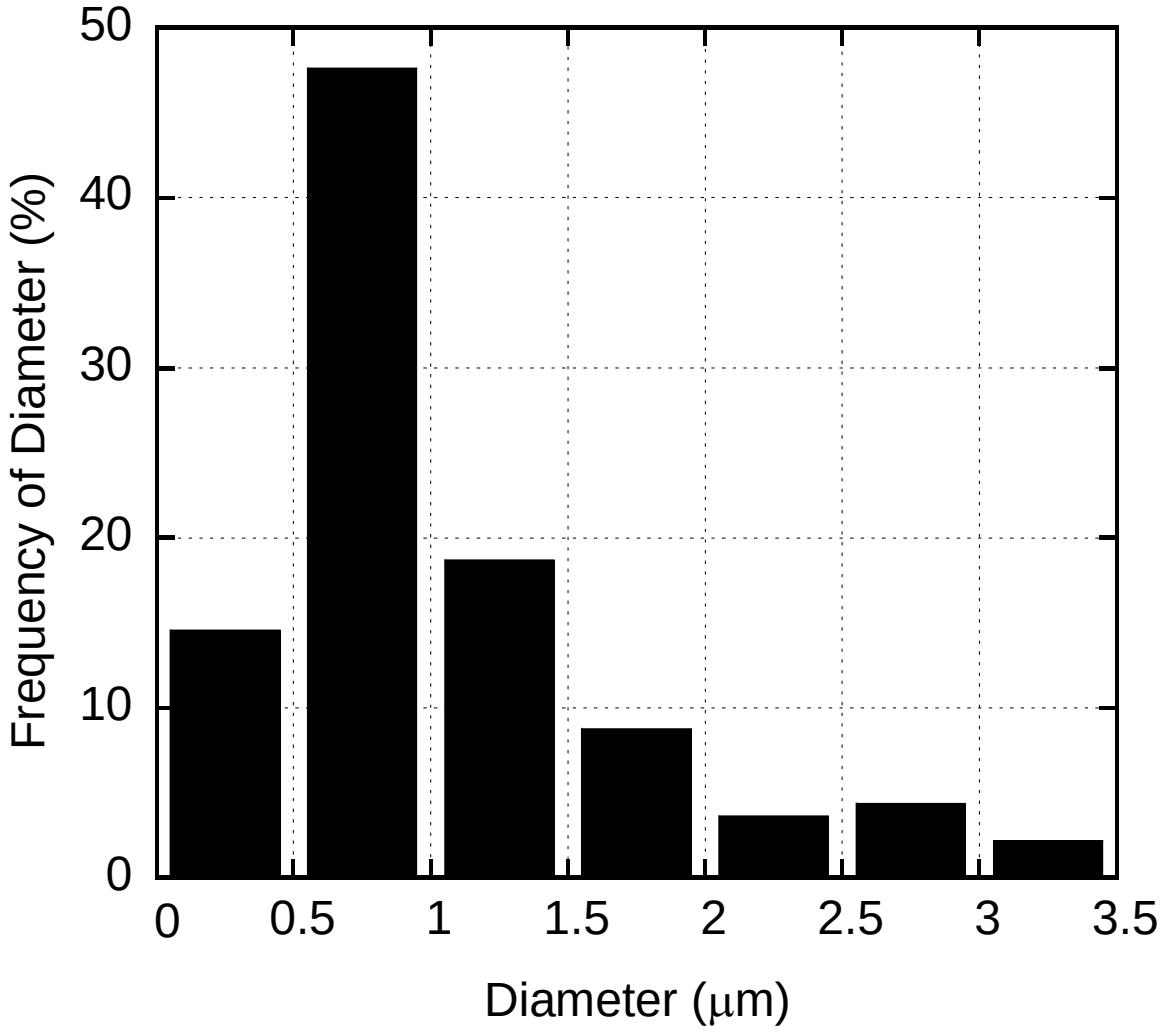

Figure 3

Vu and Yamaguchi

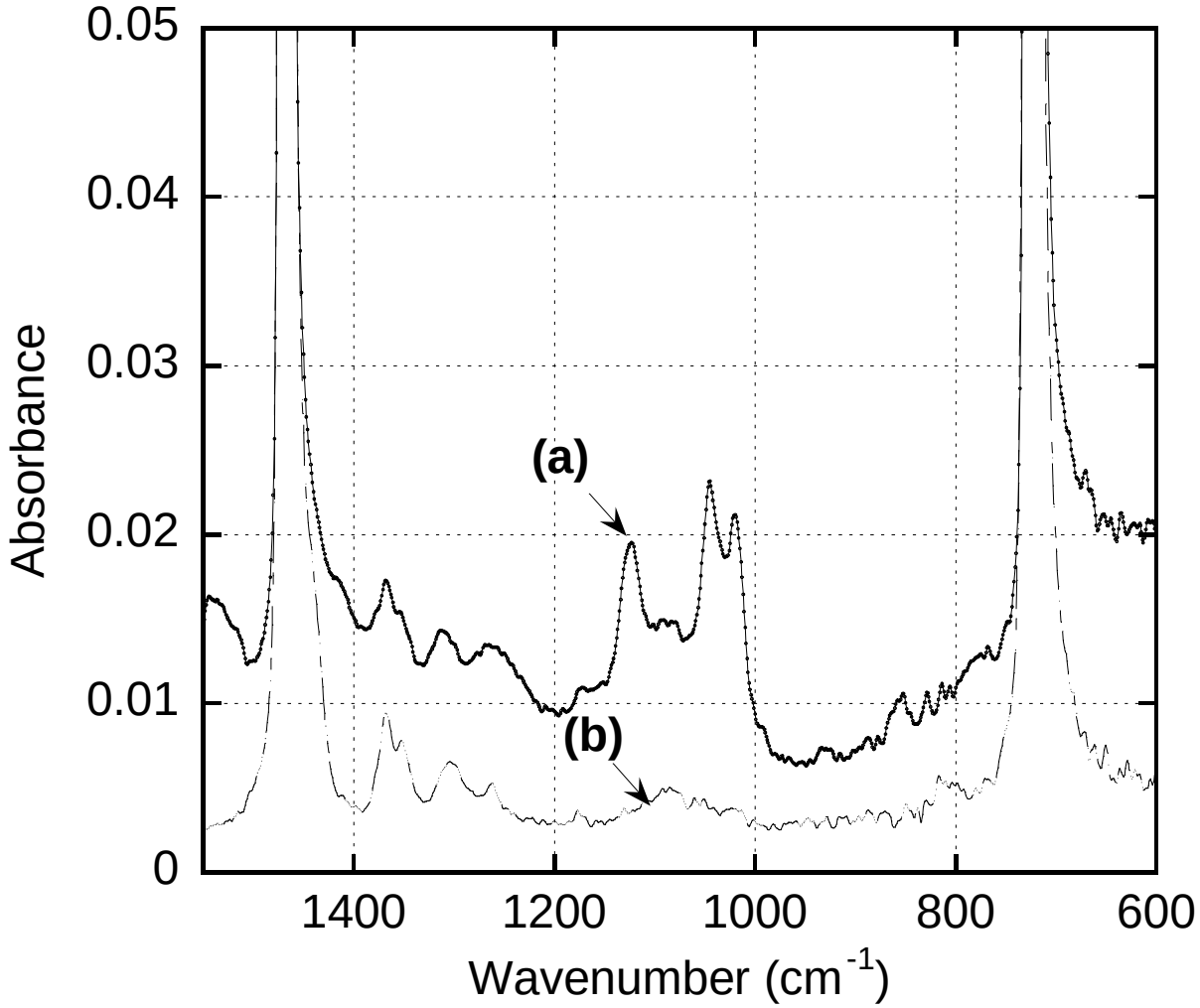

Figure 4

Vu and Yamaguchi

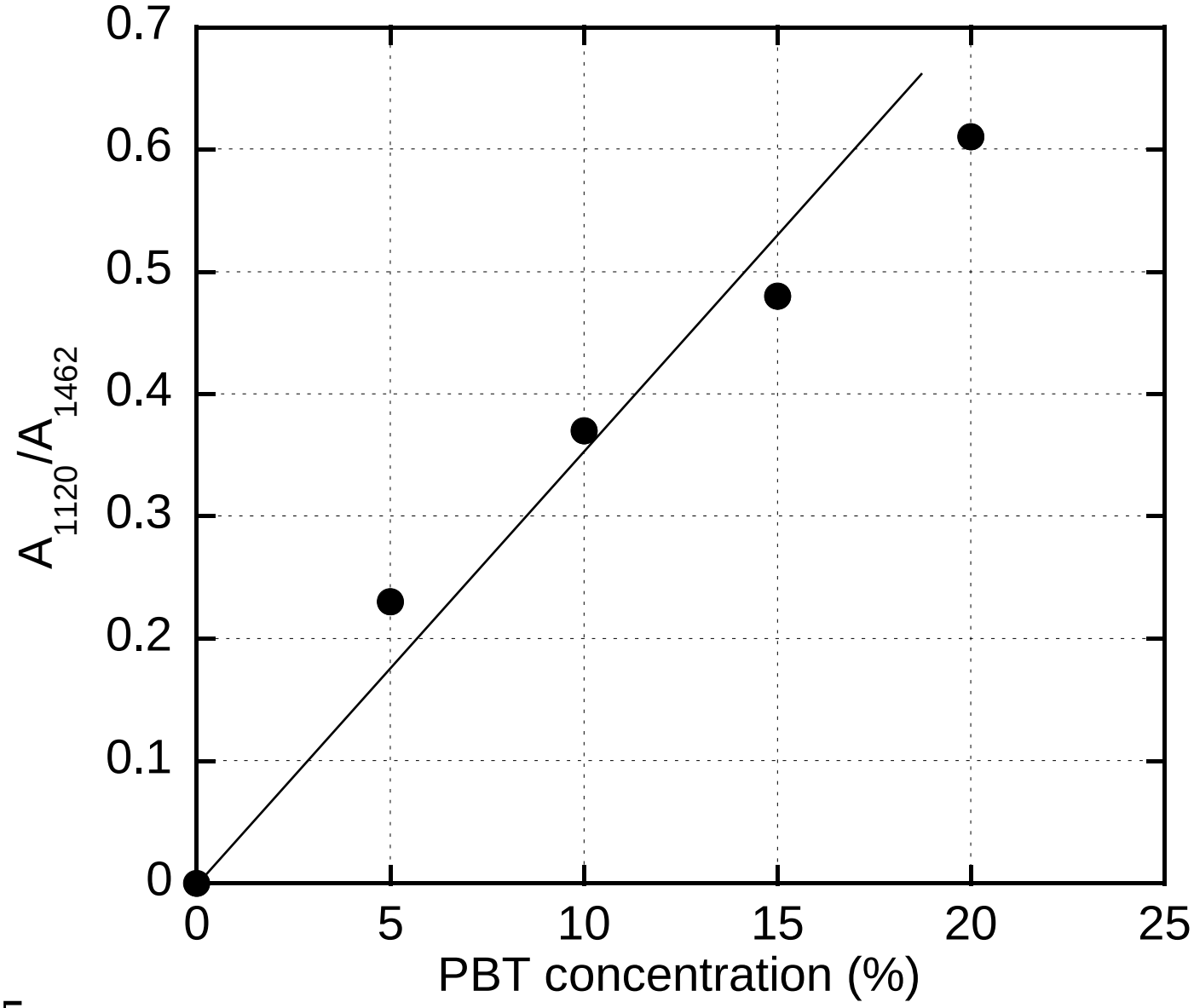

Figure 5

Vu and Yamaguchi

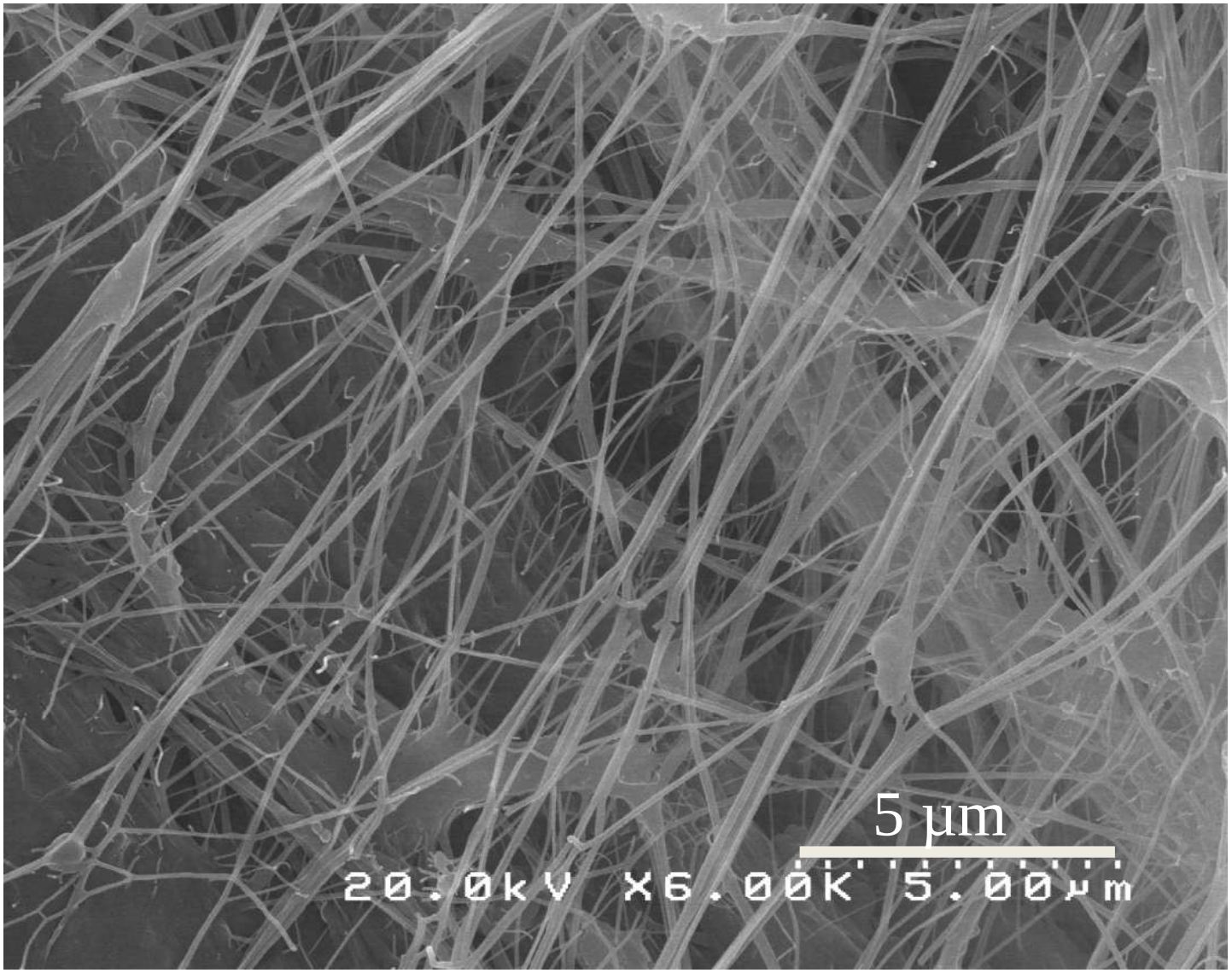

Figure 6

Vu and Yamaguchi

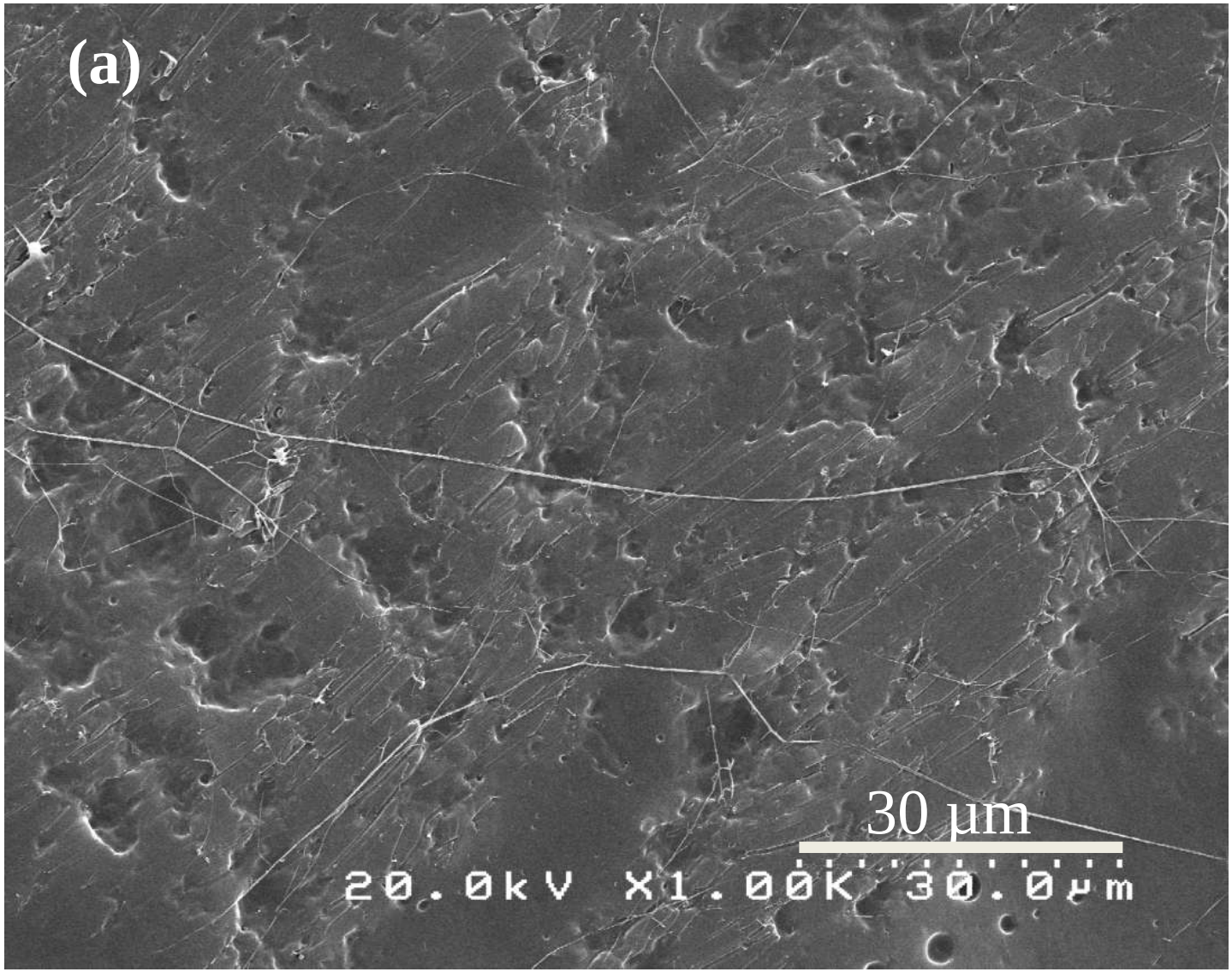

Figure 7a

Vu and Yamaguchi

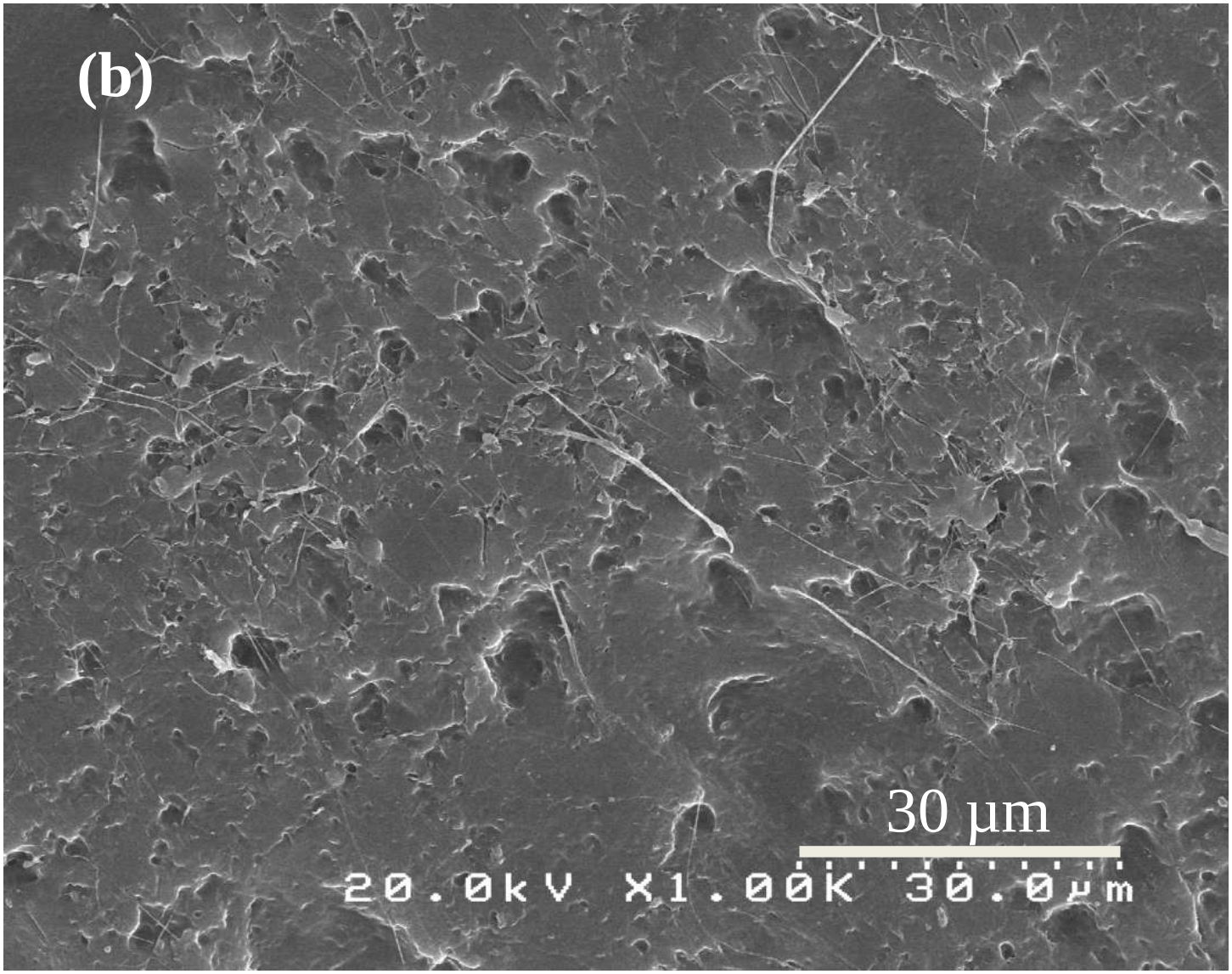

Figure 7b

Vu and Yamaguchi

Table 1: Roughness (Ra) and surface free energy of PP

Sample	Ra (μm)	Surface free energy (mJ/m^2)
Pure PP	0.03	44
PP after annealing for 5min	1.8	32
PP after annealing for 30min	1.8	29

Table 1

Vu and Yamaguchi